

TUNING OF THE FIRST SECTION OF THE BIOMEDICAL CHANNEL AT LAMPF

M. A. Paciotti, J. N. Bradbury, J. A. Helland,
R. L. Hutson, E. A. Knapp, and O. M. Rivera

University of California
Los Alamos Scientific Laboratory
Los Alamos, NM 87544

H. B. Knowles

Washington State University
Pullman, Washington

G. Pfeufer

Rice University
Houston, Texas

Summary

Results are presented from the tuning of the first section of the Biomedical Channel at LAMPF; the work centers about the use of the third bending magnet as a magnetic spectrometer. The momentum resolution at the intermediate focus is given in detail. The performance of a wedge degrader that compresses the wide momentum acceptance of the first section is discussed. The output π^- rate is also given.

Channel Description

The Biomedical Channel at LAMPF consists of eight quadrupole magnets and three wedge-type bending magnets with an intermediate focus between the second and third bends. A wedge degrader at the intermediate focus compresses a very wide momentum bite into a small momentum interval that yields a relatively narrow depth-dose distribution. Figure 1 is a view of the bend plane (X-plane) of the channel; the beam exits the channel vertically (downward) as indicated. Pions are accepted at a 70° production angle within a solid angle of about 16 msr (rms). Production targets are typically 5 cm long, 2 cm diameter cylinders of high density carbon; the 5 cm dimension determines the source size in the non-bend plane (Y-plane). The vertical size of the proton beam is the source size in the momentum resolving plane. Most of the channel tuning work was done with a 3 mm high target, fixing the bend-plane source size independently of the proton beam.

The combination BM1,2 forms in the bend plane a strongly focusing, spatially dispersive element with very little angular dispersion. Each of these two wedge magnets has normal entry and exit and is therefore very weakly defocusing in the Y-plane. With the entrance triplet de-energized the combination BM1,2 is a good broad-band spectrometer of less than 0.9% $\Delta p/p$ rms resolution with a focal plane tilted at 32° from the optic axis (Z-axis). The entrance triplet produces a small spot in the Y-plane at the wedge and an increased solid angle, at the expense of a greater X magnification from the target to the wedge.

The wedge material was selected to be Be to minimize multiple scattering. For a given Y spot size at the wedge, the Y-plane emittance is dominated by the scattering in the wedge. Both Al and Be wedges have been used, and the increased emittance of Al was apparent. The entrance face of the Be wedge was perpendicular to the entering beam and extended 13.5 cm along the X-axis. It was designed to accept $\pm 10\%$ $\Delta p/p$ of the incident momentum bite. Particles missing the wedge were absorbed by copper blocks. The wedge angle was 29.9° .

The last section of the channel constitutes a very flexible system for transporting the "source" at the wedge into fully achromatic and biologically useful beams. Along with this flexibility comes the difficulty of optimizing five quads.

Data Acquisition

The data were collected using the multiwire proportional counter (MWPC) planes indicated in Fig. 1. There are a total of 10 planes, one X and one Y plane per chamber. The signal wire spacing is 2 mm. The trigger for the system is a coincidence between the chambers 1, 2, 3, 4 and sometimes 5. Table I summarizes trigger information for the four runs used in this presentation.

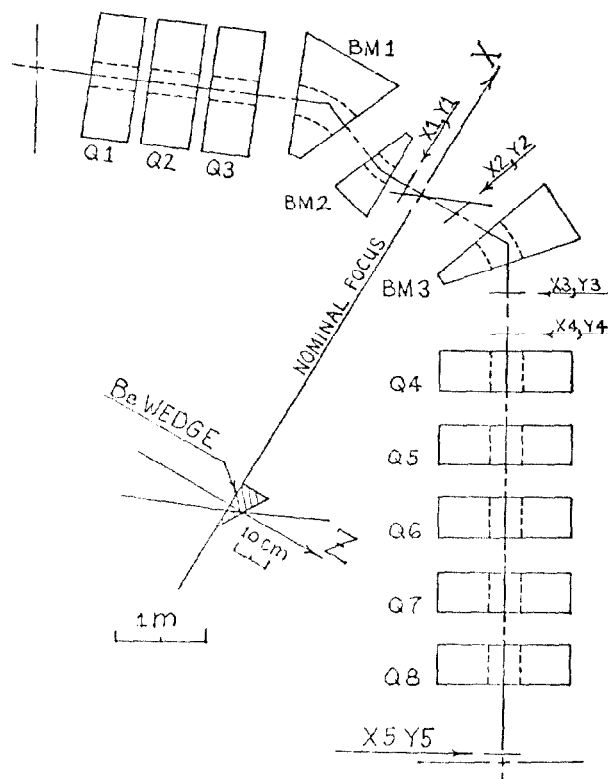


Fig. 1. Bend plane of the channel. Effective field boundaries, limiting apertures, and the location of multiwire proportional chambers are shown.

Table I

Run	Wedge	Chambers in trigger	P_0 last section	Tune of Q4-Q8
321	Out	1,2,3,4	190 MeV/c	--
338	Out	1,2,3,4,5	190 MeV/c	Design
351	In	1,2,3,4,5	171 MeV/c	Design
353	In	1,2,3,4,5	171 MeV/c	Alternate

The first section of the channel to the intermediate focus was run identically for all four runs, i.e., at 190 MeV/c with the entrance triplet tuned for optimum resolution. Presence of the wedge lowers the central momentum in the last section to 171 MeV/c.

The data collection system uses a PDP-11/45 with CAMAC interfacing. K. Klare wrote the data acquisition software.

BM3 Momentum Measurements

The last bending magnet (BM3) is a wedge magnet with a 60° bend. It has an entrance and exit poleface rotation of $+19.7^\circ$, making it a strongly focusing lens in both planes with roughly the same focal length. Magnet measurements have determined the effective length on the optic axis to be 0.4828 m and the radius of curvature of the effective edges to be +1.5 m, i.e., the field bulges out in the middle of the magnet. The TRANSPORT¹ first and second order matrix elements are used to represent BM3.

Given the particle trajectory before and after BM3, there are several ways to solve for the momentum δ_s of the particle using the matrix elements. For example, a measured angle θ downstream of BM3 can be equated to an expression that is a function of X, θ, Y, ϕ measured upstream of BM3, the TRANSPORT matrix elements, and the unknown δ_s . When a wedge is in the beam we use the X value in chamber 2 (see Fig. 1) coupled with all of the measured coordinates downstream of BM3. The calculation of δ_s from the BM3 spectrometer is made from the available chamber information. Several MWPC planes had lost efficiency by the end of the running period. The various techniques for finding δ_s have been extensively compared, using a very early run where all of the chamber planes were working, and differences between them were ~ 0.3% (rms).

Momentum Resolution

The focal plane of the channel for the optimum tune (Run 321) for the entrance triplet is tilted at an angle of 24° from the Z-axis. The predicted TRANSPORT tilt angle is 13° from the Z-axis. A polynomial fit to this measured focal plane is shown in Fig. 2. The abscissa represents the Z-axis of the channel from -40 cm to +40 cm of the nominal focal position. The ordinate is the X-axis on the same scale. The intercept of the Z-axis (+5 cm) is 4.5 cm upstream of the TRANSPORT prediction.

The focal plane is found by the following procedure: A narrow cut in δ_s of $\pm 0.5\%$ is made around a specific value of δ_s . The location in the X-Z plane is then found where the X- θ space reaches a waist. Several specific values of δ_s are taken covering the accepted spectrum, each value yielding a point on the focal plane. The difficulty is that the waist is not well defined due to aberrations in the system for large θ .

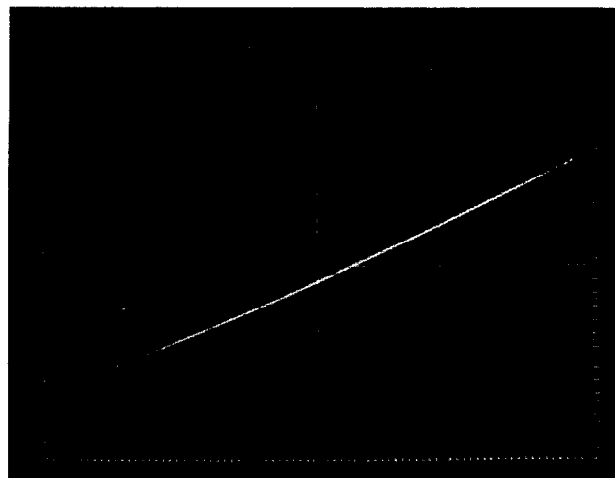


Fig. 2. Run 321, scale ± 40 cm by ± 28 cm. Focal plane of first section, tilt angle 24° .

Let X_f be the X coordinate of the point where a given particle crosses the above focal plane. Now narrow cuts are made on X_f , and the widths of the resulting distributions of δ_s are studied. The intercept and tilt of the focal plane can then be adjusted slightly to minimize the widths of the δ_s distributions. Momentum defining slits will eventually be used in a similar way to the cuts on X_f .

Once the focal plane is established, the momentum of a particle is defined by $\delta_f \equiv X_f/R_{16}$. R_{16} is the spatial dispersion and is independent of Z position since the angular dispersion is very small. The value for R_{16} found by floating wire measurements is 0.703 ± 0.007 cm/%. The distribution of X_f/δ_s has a sharp peak at 0.686 cm/% when a limiting cut is made on θ . The discrepancy between the two values is probably due to inaccurate knowledge of the matrices for the BM3 spectrometer. Figure 3, the distribution of $(\delta_s - X_f/0.686)$, gives a measure of the momentum resolution of the channel combined with that of the spectrometer. With a 15% bias² its standard deviation is 0.88%. The TRANSPORT prediction for the design channel resolution is 0.5% (rms), including the effect of He scattering at 190 MeV/c; the limiting resolution of BM3 due to finite wire spacing and multiple scattering effects is calculated to be 0.5% (rms). We can therefore say that the channel resolution lies between 0.5% and 0.7% (rms); we know of no error correlation between δ_s and X_f . The same statement is true for BM3 spectrometer resolution. Run 321 was taken at 190 MeV/c, nearly the maximum momentum of the channel, in order to minimize multiple scattering effects. Other runs were made in steps down to 140 MeV/c by scaling the entrance triplet settings from Run 321 and using floating wire measurements to provide the bending magnet settings. At 150 MeV/c the resolution function is larger by 20%, and at 140 MeV/c it is larger by 30%.

The entrance triplet was tuned to optimize the resolution function; the focal plane does not change rapidly for small variations in the triplet settings. Run 321 is the result of such an optimization.

Momentum Acceptance of Channel

The momentum acceptance of the first section of the channel plus BM3 is very broad. Figure 4 shows the momentum distribution δ_s of the beam for Run 321. No wedge degrader is present. The displacement of the centroid toward lower momenta by several percent is due in part to the fact that the higher momentum particles are more weakly focused, and their correspondingly larger

profiles are limited on the Y-apertures of the bending magnets. Not all of the particles in Fig. 4 are accepted by the last five quadrupoles of the system. Figure 5 gives δ_s for those particles in Fig. 4 that are accepted by the last section of the channel set to the design tune.

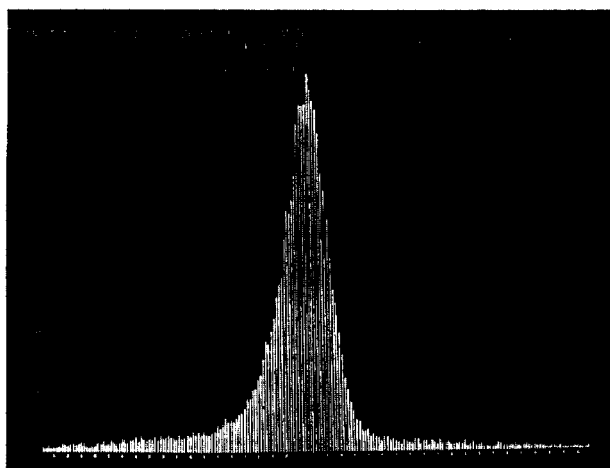


Fig. 3. Run 321, scale $\pm 10\%$. Combined resolution function of channel and BM3, $(\delta_s - X_f/0.686)$.

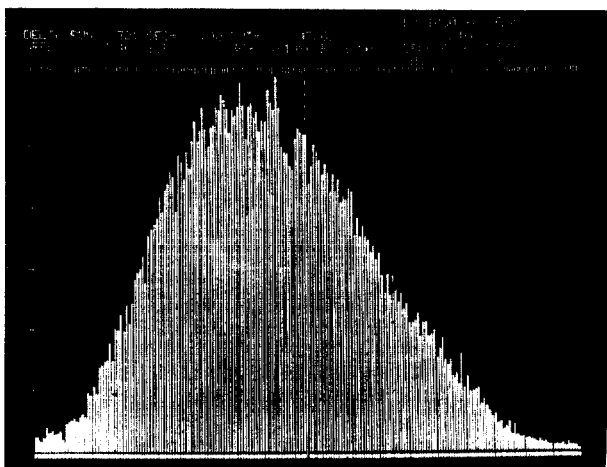


Fig. 4. Run 321, scale $\pm 20\%$, center 190 MeV/c. Momentum acceptance of channel through BM3.

It is more difficult to find the momentum acceptance of the system when a wedge degrader is present. The effect of the wedge can be computationally unfolded knowing the path length that each pion traversed through the Be wedge. Pions were separated from muons and electrons by the time-of-flight technique. One scintillator at the end of the channel provided a start pulse, and a second scintillator near the wedge provided a stop pulse. These data are shown in Fig. 6. The vertical line (1's) marks the location of a cut made to separate the large peak of pions from muons and electrons. Given the pion momentum determined from BM3, and the path length through the wedge geometrically determined from measured coordinates, the original pion momentum δ is found; this distribution is shown in Fig. 7.

As a measure of how well the unfolding process is done, the resolution function plotted in Fig. 3 is repeated, substituting the unfolded δ for δ_s ; Fig. 8 is the result. Again with a 15% bias,² its standard deviation is 1.09%, a value comparing favorably with the earlier 0.88%. The accuracy of the unfolding process is limited by the effects of multiple scattering and straggling in the original wedge traversal.

The settings of the last five quads markedly affect the shape of the momentum acceptance. Figure 9 is the unfolded δ distribution with Q4-Q8 set for an alternate tune.

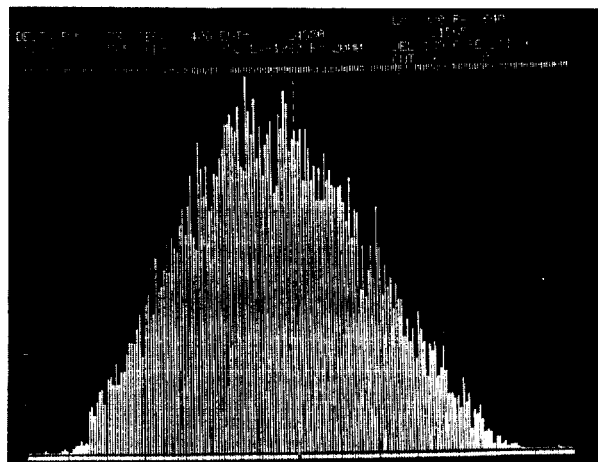


Fig. 5. Run 338, scale $\pm 20\%$, center 190 MeV/c. Momentum acceptance of entire channel without a wedge degrader.

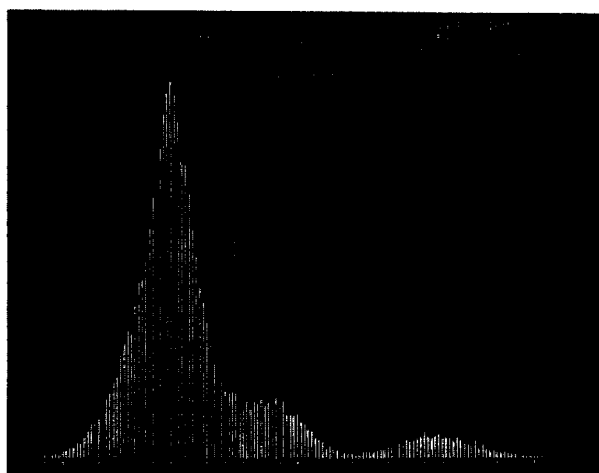


Fig. 6. Time-of-flight distribution showing pions, muons, and electrons.

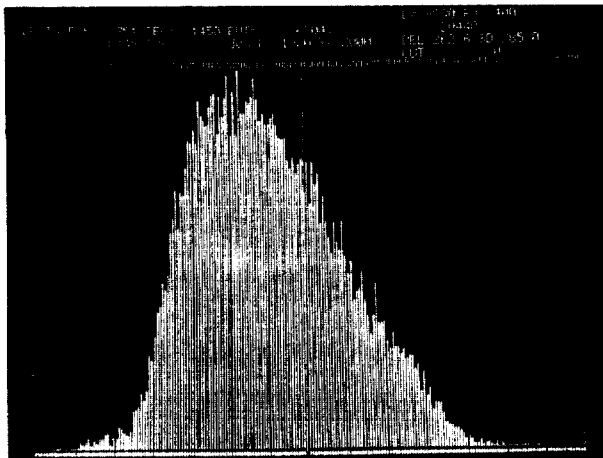


Fig. 7. Run 351, scale $\pm 20\%$, center 190 MeV/c. Momentum acceptance of channel with a wedge degrader and design settings for Q4-Q8; δ is calculated by unfolding the effect of wedge.

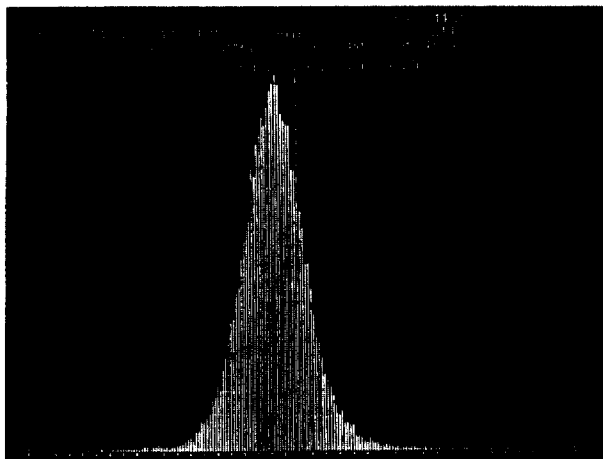


Fig. 8. Run 351, scale $\pm 10\%$. Combined resolution function ($\delta - X_F/0.686$) where δ is calculated by unfolding the effect of wedge.

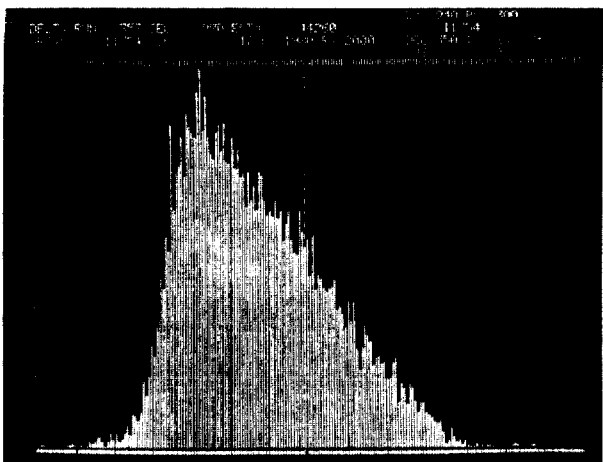


Fig. 9. Run 353, scale $\pm 20\%$, center 190 MeV/c. Momentum acceptance of channel with a wedge degrader and alternate settings for Q4-Q8; δ is calculated by unfolding the effect of the wedge.

Momentum Spectrum Out of Wedge

In the previous section the starting point for the unfolding process was δ_S , the actual measured momentum distribution of pions leaving the wedge. These δ_S spectra are given in Figs. 10 and 11 for Runs 351 and 353, respectively. (The only difference between Run 351 and Run 353 is the tuning of the last 5 quadrupoles.) With a 15% bias² the standard deviation of these plots are 1.45% $\Delta p/p$ and 1.31% $\Delta p/p$, respectively. The standard deviations of δ_S out of the same Be wedge measured early in the channel tuning period were close to 3%. At that time the air in the first section of the channel was a large contributor to loss of resolution.

By starting with a run taken without a wedge and reversing the unfolding process described earlier, the effect of the wedge can be simulated. Time-of-flight data are unavailable for a wedge out run, and every particle was assumed to be a pion. Energy loss straggling effects are included for each particle tracked through the simulated wedge. Range changes due to multiple coulomb scattering have not been included, nor has the effect of interactions been simulated.

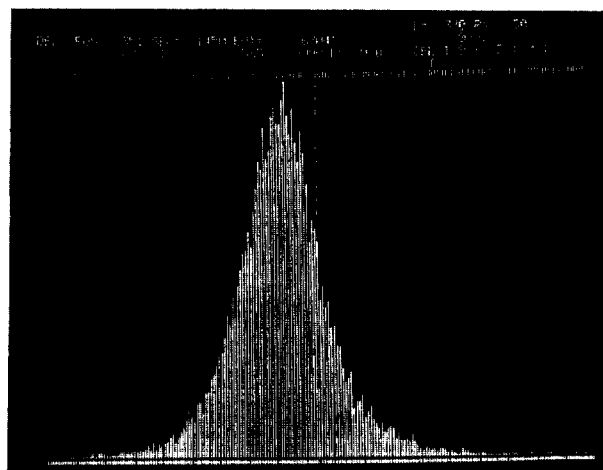


Fig. 10. Run 351, scale $\pm 10\%$, center 171 MeV/c. Measured δ_S spectrum out of Be wedge.

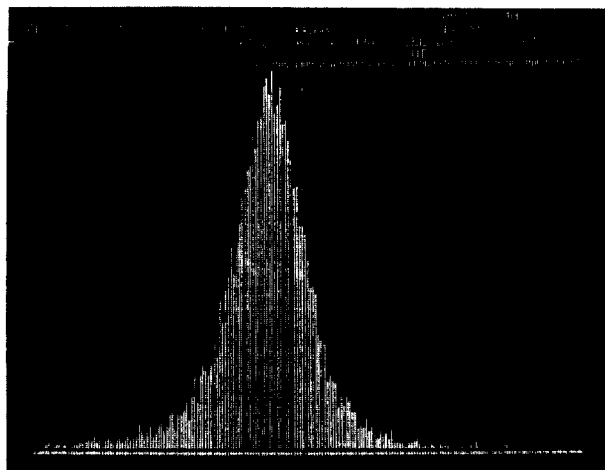


Fig. 11. Run 353, scale $\pm 10\%$, center 171 MeV/c. Measured δ_S spectrum out of Be wedge.

We begin by simulating the effect of the wedge on the particles in Runs 321 and 338. The wedge accepts $\pm 10\%$ $\Delta p/p$, and those particles that are dispersed so as to miss this wedge are cut out, i.e., the value of X at the face of the wedge is limited to ± 6.5 cm. This cut removes about 20% of the available flux. Figure 12 shows the δ distribution out of the simulated Be wedge for Run 321; a 15% bias² gives a standard deviation of 1.42% $\Delta p/p$. This spectrum should be compared with Fig. 10 or 11. Figure 13 is the measured δ_s , a repeat of Fig. 4 with a 20% loss of events that miss the wedge. Figures 14 and 15 are the corresponding simulated δ and the measured and cut δ_s distributions for Run 338. Run 338, with its trigger at the end of the channel, has considerably less background. The simulated δ 's (Figs. 12 and 14) are to be compared directly with the above-mentioned measured δ_s distributions coming out of the same wedge (Figs. 10 and 11).

Confidence in accurate wedge simulations allows one to design different wedges and to then determine the resulting momentum spectrum. Presently we are accepting $\pm 10\%$ $\Delta p/p$ into the wedge and rejecting the rest of the spectrum. It may be desirable to accept more or less of the spectrum.

Optimization of the Be wedge was studied for the low background Run 338. Wedge position in Z was varied; wedge angle was varied to reduce residual X - δ correlation; and wedge tilt angle was varied. On first thought one might tilt the wedge toward the focal plane to take advantage of the best resolution there. In this case positive θ pions penetrate more Be than negative θ pions with the same X_f . This effect can be somewhat offset by moving the wedge upstream, in which case the positive θ pions will traverse the wedge at a lesser value of X and therefore see less material. A balance of these effects and an improved δ distribution was obtained for a wedge whose entrance face was tilted 35° toward the focal plane and at the same time moved upstream by 5 cm. The improvement in the width of the δ spectrum is however, less than 10% when the effects of straggling are included.

Target to Wedge Magnification

The X -plane magnification from the target to the wedge can be measured easily with our target insertion mechanism. Targets are inserted vertically and can be moved up and down in a controlled fashion; a 1 cm motion of the tuning target was used. The X motion of the beam spot at the nominal focus was measured while a narrow, fixed cut on δ_s was made as well as limiting cuts on θ , Y , and ϕ at the intermediate focus. The magnification was found to be ~ 0.7 , somewhat smaller than the TRANSPORT prediction of ~ 1.13 . The magnification is a basic property of the channel, and we expect to study this discrepancy with a Monte Carlo simulation of the channel.

The vertical proton spot on our target is expected to be 0.3 cm rms. With a magnification of ~ 0.7 , an additional contribution of 0.3% is to be folded in with the resolution width. This effect will not significantly change our reported results when a large target is used unless the design proton beam size on the target cannot be achieved.

Rate Measurements

Channel rate measurements have been made for target-to-wedge magnifications in the X -plane ranging from ~ 0.2 to ~ 2.5 and from 0.5 to 2.5. The entrance triplet settings are taken from TRANSPORT solutions for each magnification with point-to-point imaging in both planes from target to wedge. The Be wedge was in place,

and Q4-Q8 were set to the design tune when rates were measured with a scintillator at the end of the channel. The channel rate increases with increasing magnification magnitude, reaching about equal maxima at ~ -2.0 and $\sim +2.0$ X -magnification. Resolution optimization for a given magnification was found to require lower entrance triplet settings and consequently produced lower rates.

The rate at the end of the channel for Run 351 is 1.3×10^6 π^-/s per μA of protons on a 5 cm carbon target with density 1.9. This rate is 75% of the maxima found above. We measured 20% of the beam to be muons and electrons, and this correction has been applied. The proton beam was monitored with a scintillation detector operated in a current (rather than pulse counting) mode. The detector was positioned at the end of a hole in the shielding, viewing the target at 110° . The proton beam intensity was reduced by a factor of approximately 200 by use of a collimating beam stop upstream in order to reduce the proton current to an acceptable 0.2 μA peak. This situation made the calibration of the proton beam uncertain to $\pm 25\%$. The rate prediction for Run 351 is 1×10^6 π^-/s - μA .

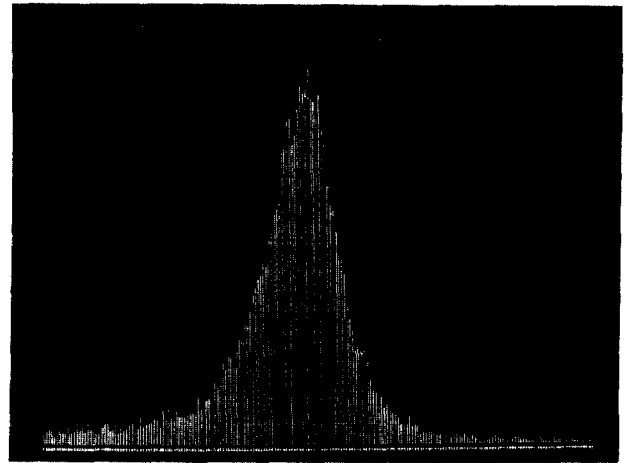


Fig. 12. Run 321, scale $\pm 10\%$, center 171 MeV/c. Calculated δ spectrum out of simulated Be wedge.

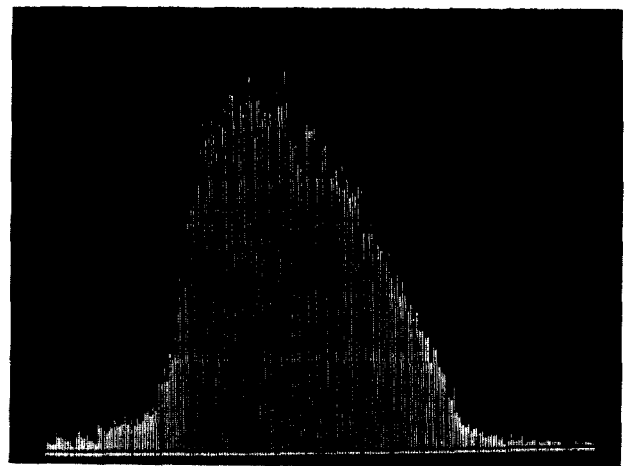


Fig. 13. Run 321, scale $\pm 20\%$, center 190 MeV/c. Momentum spectrum accepted into the simulated Be wedge.

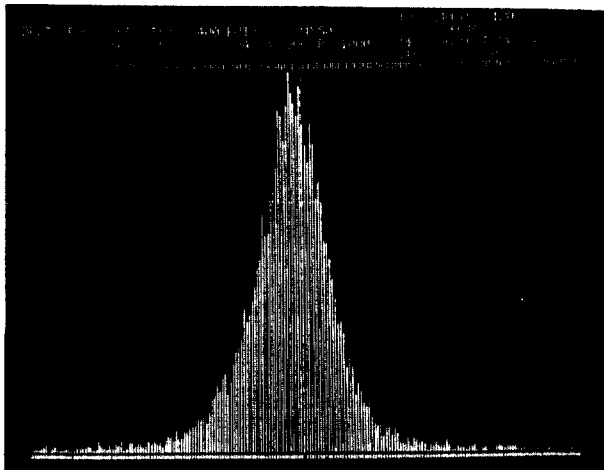


Fig. 14. Run 358, scale $\pm 10\%$, center 171 MeV/c. Calculated δ spectrum out of simulated Be wedge.

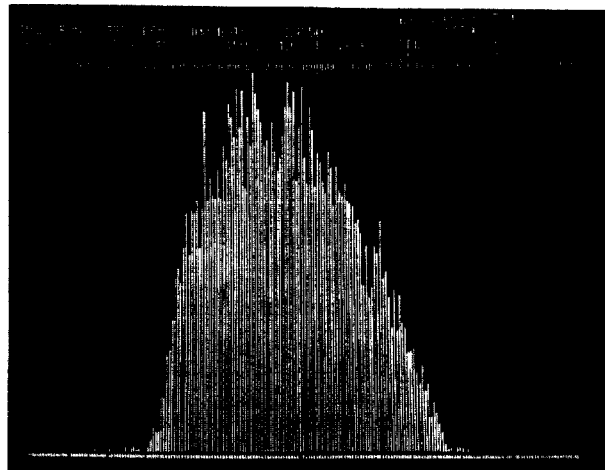


Fig. 15. Run 338, scale $\pm 20\%$, center 190 MeV/c. Momentum spectrum accepted into the simulated Be wedge.

References

1. K. L. Brown and S. K. Howry, "TRANSPORT/360, A Computer Program for Designing Charged Particle Beam Transport Systems," SLAC-91 (1970).
2. H. Koziol provided us with a method to eliminate the effects of the large tails that accompany all of our gaussian-like distributions. The "bias" is a lower limit given as a percentage of the peak height. The standard deviation of the distribution above this lower limit is then divided by the standard deviation of the true gaussian $e^{-x^2/2}$ above the same fractional lower limit. In effect, non-gaussian tails are replaced by gaussian ones.